

Integrated microsystem for dielectrophoretic cell concentration and genetic detection

Eric T. Lagally, Sang-Ho Lee and H. T. Soh*

Received 27th April 2005, Accepted 16th August 2005

First published as an Advance Article on the web 31st August 2005

DOI: 10.1039/b505915a

We have directly integrated a continuous-flow, electrokinetic method of bacterial cell concentration with room temperature, sequence-specific genetic detection. The system we have developed traps cells from a continuous-flow sample stream *via* dielectrophoresis, providing a 160-fold increase in cell concentration. PDMS microvalves then define a 100 nL volume around the trapped cells to which cell lysis buffer and genetic detection components are introduced. Direct, optical detection of *Escherichia coli* MC1061 cells is then accomplished *via* the sequence-specific hybridization of an rRNA-directed optical molecular beacon. This integrated microsystem is capable of sequence-specific genetic detection of 25 cells within 30 min.

Introduction

The rapid, high-sensitivity detection and genetic analysis of bacterial cells remains an important goal of biotechnology. The many diagnostic applications of systems capable of performing such detection, such as the detection of infectious agents, have led to the development of a wide variety of microsystems for the differentiation and detection of bacterial pathogens.^{1–6} The potential impact of such systems has been further enhanced by the Microbial Genome Project,⁷ which has significantly increased the availability of genetic data for pathogenic bacteria. This has resulted in the availability of a wide range of species-specific, serotype-specific, and strain-specific markers for genetic detection. Nevertheless, our ability to detect pathogens at extremely low concentrations remains limited, which is a critical handicap in the early detection of pathogens. For example, as few as 50 cells of *E. coli* O157:H7 is sufficient to cause infections, and these 50 cells may be spread across a large area or be diluted in a large volume.⁸ Thus the development of biosensors sufficiently sensitive to detect such low cell concentrations has received much attention. Here, in contrast, we present an alternative and complimentary solution to this problem. Instead of improving sensor sensitivity, we demonstrate an electrokinetic technology for rapidly increasing the concentration of bacteria integrated with the genetic analysis.

Several groups have previously pursued cell concentration on the microscale. For example, Cabrera and Yager presented a microfluidic flow cell for bacterial concentration utilizing electrokinetic effects,⁹ and Grodzinski and coworkers presented a microfabricated system for cell concentration and genetic sample preparation from complex sample backgrounds.¹⁰ In order to reap the full benefits of such a sample concentration, however, the microsystem should be integrated with a means of genetic detection. Currently, we are not aware

of any prior work that has demonstrated the feasibility of on-chip concentration followed by direct, on-chip genetic detection. For example, Lagally and others have described portable systems for differentiation and detection of bacterial pathogens including PCR amplification, and microchannel capillary electrophoresis (CE) detection,^{2,3,6} yet none of these systems included a method for integrated isolation and concentration of bacterial pathogens. This limits their use to pathogen concentrations of thousands of cells mL⁻¹.

Our device uses PDMS microvalves to define a chamber volume around a set of microelectrodes. By closing the microvalves after trapping bacterial cells in the sample in a continuous-flow manner, we greatly reduce the volume and therefore greatly enhance the locally detectable concentration of genetic material. Our microsystem utilizes an optical molecular beacon dissolved in a high concentration of a chaotropic salt to lyse the bacteria and to conduct rapid sequence-specific hybridization to detect the presence of 16S ribosomal RNA from *Escherichia coli* cells.

Dielectrophoresis

Dielectrophoresis (DEP) is a force on charge neutral particles in a non-uniform electric field arising from differences in dielectric properties between the particles and the suspending fluid. The time-averaged force on a homogeneous sphere of radius r_p can be approximated as:

$$\vec{F}_{\text{DEP}} = 2\pi\epsilon_m r_p^3 \text{Re}(K) \nabla |E_{\text{rms}}|^2 \quad (1)$$

Here $\text{Re}(K)$ is the real part of K , the Clausius–Mosotti factor, defined as:

$$K = \frac{\epsilon_p^* - \epsilon_m^*}{\epsilon_p^* + 2\epsilon_m^*} \quad (2)$$

where ϵ_p^* is the complex permittivity of the particle and ϵ_m^* is the complex permittivity of the medium. Trapping of certain cell types may be achieved by specifically attracting them to electrodes (positive K) while repelling others (negative K).¹¹ In the case of bacteria, and *E. coli* in particular, the cross-over

California Nanosystems Institute and Department of Mechanical and Environmental Engineering, University of California—Santa Barbara, Santa Barbara, CA 93106, USA. E-mail: tsoh@engineering.ucsb.edu; Fax: +1 (805) 893-8651

frequency is reported to be a stronger function of medium permittivity than frequency. For media with conductivities smaller than the measured conductivity of the cell ($\sigma \approx 44 \text{ mS m}^{-1}$), K is positive for frequencies smaller than about 1 MHz.^{12,13} For mammalian cells, however, the cross-over frequencies from negative to positive K are better defined, and typically lie in the range between 10 and 90 kHz.¹¹ Therefore, by setting the DEP frequency below the cross-over frequency of non-bacterial cells and operating in a medium with sufficiently low permittivity, selective capture of bacteria is possible while rejecting larger cells in the sample.

Materials and methods

Cell lysis buffer and molecular beacon design

Guanidine thiocyanate (GuSCN), *N*-laurylsarcosine, 1 M Tris-HCl, and 0.5 M EDTA were purchased from Sigma. All buffer components were nuclease-free and all dilutions were performed into nuclease-free water or buffer. The cell lysis buffer stock solution consisted of 60 mM Tris, 12.25 mM EDTA, 5 M GuSCN, and 1% *N*-laurylsarcosine. The stock solution was diluted to a final concentration of 50 mM Tris, 10 mM EDTA, 4 M GuSCN, and 0.8% (w/v) sarcosine for all experiments.

The molecular beacon had the sequence 5'-CCA CGC CTC TTT GGT CTT GCG ACG TGG-3' and contained a 5' Rhodamine Red-X fluorophore¹⁴ and a 3' Black Hole-2 quencher (Integrated DNA Technologies, Coralville, IA). Complementary target DNA oligonucleotides were provided with the beacon. The beacon sequence was chosen to be fully complementary to a section of the 16S rRNA gene from *Escherichia coli* K12 (Genbank accession #AF233451) using the BioEdit sequence alignment editor.¹⁵ The lyophilized beacon was resuspended to a stock concentration of 100 nM in 1× Tris-HCl EDTA buffer (1× TE, pH 7.6). Aliquots of the stock solution were diluted 1 : 10 in the cell lysis buffer to form the working concentration of 10 nM.

Bacterial culture and dilution

Escherichia coli MC1061 cells transformed with a plasmid containing the gene for green fluorescent protein under the control of the arabinose promoter¹⁶ and conferring resistance to chloramphenicol (CM) were grown overnight at 37 °C on agar plates. Colonies were picked from the plates and suspended in minimal LB broth with 25 $\mu\text{g mL}^{-1}$ CM (Sigma, St. Louis, MO) and grown overnight at 37 °C. For cells expressing green fluorescent protein, this culture was then subcultured 1 : 50 into fresh minimal LB broth with 25 $\mu\text{g mL}^{-1}$ CM and grown for 2 h. Expression of green fluorescent protein was induced by adding 0.02% arabinose to the culture media and growing overnight at 37 °C. Cell density was quantitated by optical density determination of the broth/cell suspension at 600 nm with a spectrophotometer (Biophotometer, Eppendorf, Westbury, NY). The spectrophotometer was calibrated by plating serial dilutions of cell suspensions onto LB agar plates and growing overnight at 37 °C. Colony-forming units were counted and a calibration curve of optical density *versus* cell concentration was established.

To prepare cells for analysis, a 1 mL aliquot of the cell culture was washed by threefold centrifugation for 5 min at 5000 rpm in a tabletop centrifuge followed by resuspension in nuclease-free 1× phosphate buffered saline (1× PBS). Dilutions of this suspension were made into nuclease-free 0.01× PBS (conductivity 30 mS m^{-1}), which served as the cell capture buffer.

Device design and fabrication

The mask design for the microsystem is presented in Fig. 1. Two independent inlet channels connect through a series of PDMS microvalves to a common central cell capture channel. The cell capture channel (167 μm wide, 100 nL in volume) contains a set of interdigitated electrodes (20 μm width, 20 μm spacing), which are powered with AC frequencies to establish a dielectrophoretic force on bacteria in the sample stream. Filtered sample passes through a PDMS microvalve at the end of the capture channel to waste. The microvalves are similar to those described by Grover *et al.*¹⁷ The dead volumes of these microvalves are 50 nL each.

To form the microchannels, a 0.55 mm thick, 100 mm diameter glass wafer (University Wafers, South Boston, MA) was cleaned and a 200 Å layer of chrome was deposited on one side using electron beam evaporation. The chrome was used to form a reflective surface for optical alignment of both

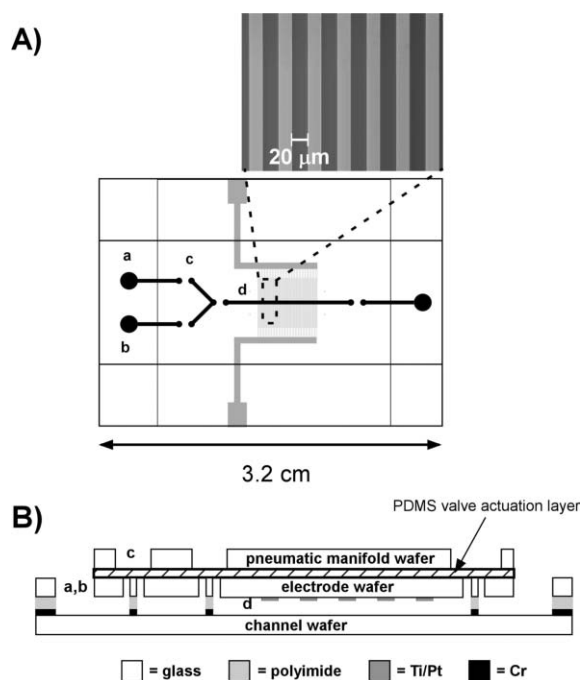


Fig. 1 (A) The mask design for the integrated cell concentration and genetic analysis microsystem. Cells are introduced through the top reservoir and channel at (a), proceed through PDMS microvalves (c) to the chamber (d). Cells are trapped on the electrodes (inset, 20 μm width, 20 μm spacing). Waste exits the chamber through a PDMS microvalve to the waste reservoir. After cell capture, cell lysis solution with the molecular beacon is introduced at reservoir (b) and flowed until it fills the chamber. (B) Side view of the microsystem illustrating the relative orientation of the substrates, polyimide layers, and electrodes.

substrates during the flip-chip bonding process. Following deposition, a 40 μm -thick layer of photopatternable polyimide (HD-4010, HD Microsystems, Cupertino, CA) was spun onto the chrome and baked for 3 min at 65 $^{\circ}\text{C}$ on a hotplate, then baked for 5 min at 105 $^{\circ}\text{C}$ on a hotplate following a 3 min relaxation. The film was left to relax for 30 min at room temperature. Next, the polyimide was exposed with the channel mask using a contact aligner (MJB3, Karl Suss, Waterbury Center, VT). The exposed wafer was left in the dark at room temperature for 2 h to fully crosslink, and was then developed in polyimide developer (PA-400D, HD Microsystems) for 1.5 min, 1 : 1 polyimide rinsers : developer for 1.5 min, and rinsers for 30 s (PA-400R, HD Microsystems). The use of photopatternable polyimide reduces fabrication time compared to other fabrication platforms, such as glass or silicon subtractive fabrication methods, which require deposition and patterning of a sacrificial etch mask. In addition, the polyimide fabrication maintains chemical compatibility, temperature resistance, and hydrophilicity. To form the electrodes, a 100 mm diameter glass wafer (0.55 mm-thick, University Wafers, South Boston, MA) was cleaned and photoresist was spun on and photolithographically patterned. Following deposition of 200 \AA of Ti and 2000 \AA of Pt using electron-beam evaporation, standard liftoff was performed by sonicating the wafer in acetone for 10 min. The reservoirs and microfluidic valve vias were next drilled through the electrode wafer using a CNC mill equipped with a diamond-tipped drill bit (Flashcut CNC, Menlo Park, CA). Both the channel wafer and the electrode wafer were diced (Disco DAD-2H/6, Tokyo, Japan). Following cleaning, the resulting channel and electrode chips were aligned and lightly bonded at 300 $^{\circ}\text{C}$ for 10 min using a flip-chip bonder (Research Devices M8A, Piscataway, NJ). Next, the polyimide was fully cured by applying slight compressive force at 375 $^{\circ}\text{C}$ in a nitrogen environment for 30 min using a wafer bonder (SB6, Karl Suss).

The valves were assembled following bonding using the method of Grover *et al.*¹⁷ Briefly, a PDMS membrane (254 μm thick HT-6240, Bisco Silicones, Elk Grove, IL) was applied to the bonded device. This assembly and a diced glass manifold (1.1 mm thick borofloat glass, Precision Glass and Optics, Santa Ana, CA) were simultaneously cleaned in a UV-ozone cleaner (PR-100, UVP, Upland, CA) and then irreversibly bonded at room temperature for 2 h. To prevent nucleic acid adsorption onto the glass microchannels, the channels were coated using a modified Hjertén¹⁸ protocol.

Instrumentation

The device was controlled using a LabVIEW program (National Instruments, Austin, TX). DEP was performed at 250 Hz using the analog output from a DaqCard 6036E (National Instruments). Bacterial cell suspensions and cell lysis buffer with molecular beacon were introduced to separate inlet channels using a programmable syringe pump (PHD 2000, Harvard Apparatus, Holliston, MA). The valves were actuated using pressure and vacuum from a floor pump and were controlled using digital signals from the data acquisition card

to actuate solenoid valves in a custom-built pneumatics box. Basic fluorimetry experiments were conducted in a standard fluorimeter using a low-volume cuvette. Cell trapping experiments were performed on an epifluorescence microscope (Leica DM LS2, Bannockburn, IL) equipped with a GFP filter set with mercury arc lamp excitation using a 20 \times objective and images collected using a cooled CCD camera (ORCA ER, Hamamatsu, Bridgewater, NJ). Cell trapping, lysis, and detection experiments were performed on a laser scanning confocal microscope (Olympus Fluoview, Melville, NY) equipped with a 10 \times , 0.4 NA objective. Laser light from a 543 nm solid-state diode laser was focused onto the microchannel and fluorescence was collected in a line scan mode and compiled into images using the Olympus Fluoview software.

Image analysis was conducted using ImageJ software. Confocal fluorescence images were saved as 16 bit TIFF images, and the threshold was calibrated at the level of the image with the maximum fluorescence. Regions of interest (ROIs) of a consistent size (200 \times 300 pixels) were defined across all images, and average pixel values were calculated. Three ROIs were defined for each image, and the arithmetic mean of pixel intensity values across all three ROIs were calculated and used as the fluorescence intensity. Uncertainty values were obtained by calculating 2 standard deviations in pixel intensity across all three ROIs for each image and subsequently calculating the arithmetic mean of these values to obtain a single uncertainty value for each image.

Results and discussion

Microsystem design

The integrated microsystem presented here was designed to capture bacterial cells using positive dielectrophoresis, and then to reduce the volume surrounding the captured cells so that a genetic detection is performed at increased local analyte concentrations. The microelectrode design, as presented in the photograph in Fig. 1, was optimized using finite-element modeling (data not shown) to maximize DEP capture at flow rates of 100 $\mu\text{L h}^{-1}$. The optimized electrode dimensions for these experiments were 20 μm electrode widths with 20 μm spacing. Using this microelectrode spacing, we successfully trapped green fluorescent protein (GFP)-expressing *E. coli* bacteria from a continuous-flow sample stream. Fig. 2A presents a fluorescence microscopy image of our microelectrodes after 10 min of cell flow (100 $\mu\text{L h}^{-1}$) at a concentration of 10⁵ cells mL^{-1} with the microelectrodes in an unpowered state. No cells are visible on the microelectrodes. Fig. 2B presents a fluorescence microscopy image of the same electrodes after 10 min of cell flow while applying 7 Vpp (Volts peak-to-peak) at a frequency of 1 kHz. Numerous GFP-expressing *E. coli* cells can be seen trapped on the microelectrodes. Bacterial cell trapping was successful at flow rates of 100 $\mu\text{L h}^{-1}$ for peak-to-peak voltages above 7 V and frequencies below 10 kHz. The electrolysis potentials for the cell suspension buffer at 1 kHz and 250 Hz were 13.8 Vpp and 9 Vpp, respectively. These results indicate we would be able to operate our microsystem at higher flow rates than those presented here.

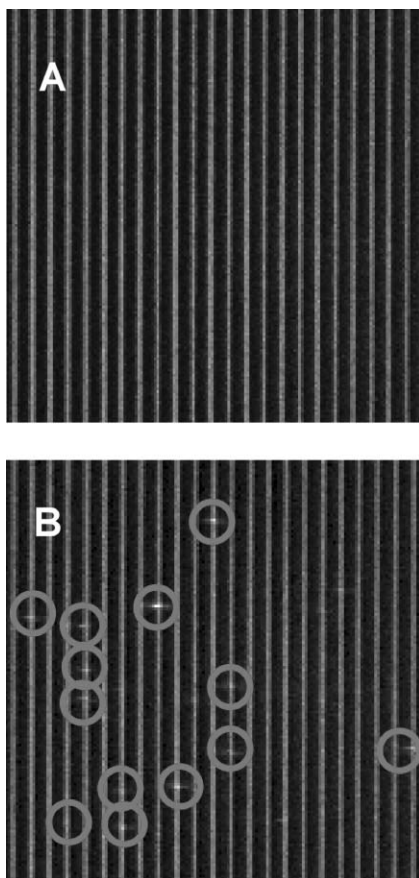


Fig. 2 (A) An epifluorescence image taken after 10 min of cell flow over the interdigitated microelectrodes without DEP voltage applied. Non-specific binding does not occur and no cells are visible. (B) The same microelectrodes after 10 min of flow with 7 V applied at 1 kHz. Cells are captured by DEP onto the electrodes.

Optical molecular beacon design

We chose to use an optical molecular beacon to detect the presence of ribosomal RNA from *E. coli*. Some strains of *E. coli* are pathogenic,¹⁹ and it serves as a good model organism for the generalized detection of bacterial pathogens of many types. The size of *E. coli* cells is consistent with those of other pathogenic bacteria, and others have shown that multiple types of pathogens share similar dielectric responses when acted on by AC fields.²⁰ We desired a detection method that would be sequence-specific, and that could be conducted within 30 min at room temperature, negating the need to heat the device. The chaotropic salt, GuSCN, was chosen as the reagent for cell lysis and endonuclease denaturation. In addition, it serves an important secondary function to increase the hybridization speed at room temperature by lowering the melting temperature of nucleic acid hybrids.^{21–23} We designed our molecular beacon to operate in high concentrations of chaotropic salt by increasing the melting temperature of the stem region to increase stability in the folded state. Our choice of fluorophore and stem sequence took into account the effects of contact quenching between different fluorophores and standard fluorescence quenchers²⁴ as well as efforts to maximize solubility and minimize hydrophobicity.²⁵

Additionally, our choice of fluorophore was based on the absorption maximum at wavelengths longer than 550 nm, since certain cell components as well as the polyimide used in fabrication fluoresce when excited by wavelengths below 500 nm.²⁶

To test the performance of our molecular beacon, we conducted a series of fluorimetry experiments to measure fluorescence of the molecular beacon in the presence and absence of a fully complementary DNA oligonucleotide target. Fig. 3 presents the normalized fluorescence intensity of our molecular beacon in the presence and absence of target, in both standard 1 × TE buffer as well as our cell lysis buffer including a high concentration of GuSCN. The molecular beacon responds to an excess of target by hybridizing fully with the target and increasing its fluorescence above background in the presence of both buffers. The addition of 4 M GuSCN has minimal effect on the maximum fluorescence, as indicated by the nearly overlapping spectra in both buffers.

We next conducted experiments to determine hybridization rate between the molecular beacon and its target sequence by adding a 100-fold excess of complementary DNA to the molecular beacon in the presence of 1 × TE and 4 M GuSCN. Fig. 4 presents the normalized fluorescence of the molecular beacon/target system as a function of time. The molecular beacon responds quite slowly to even an excess of target when dissolved in 1 × TE, taking almost 40 min to reach 50% of the fluorescence maximum. When the beacon is dissolved in 4 M GuSCN cell lysis buffer, however, the fluorescence reaches its maximum immediately, and is stable over the

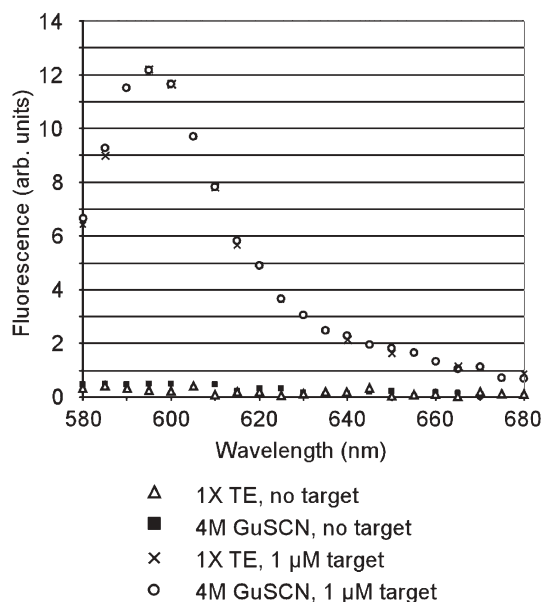


Fig. 3 The fluorescence response of 10 nM molecular beacon in various buffers in an excess (1 μM) and absence of oligonucleotide DNA target. The molecular beacon demonstrates low background in both 1 × TE buffer and 4 M GuSCN chaotropic salt. The fluorescence increases to its maximum upon the addition of excess DNA oligo. The similarity of the fluorescence spectra for the molecular beacon in both buffers indicates that the GuSCN has no detrimental effect on beacon fluorescence or fluorescence background.

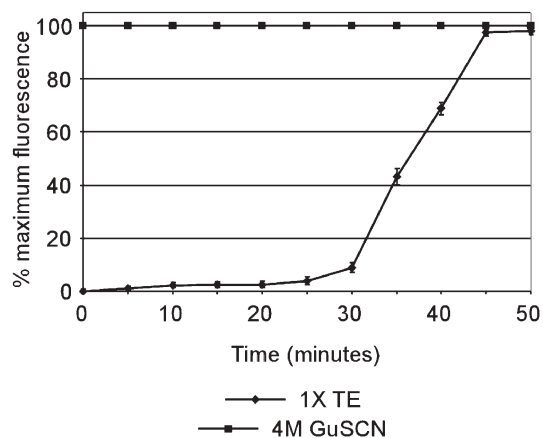


Fig. 4 The time response of the molecular beacon hybridizing to an excess of DNA oligonucleotide target (1 μM). In $1\times$ TE buffer, the hybridization proceeds over a time of approximately 40 min. In the GuSCN buffer, however, the hybridization is immediate and the maximum fluorescence is observed immediately and is stable for the entire measurement period.

entire measurement period. The fluorescence of the same beacon in 4 M GuSCN without target demonstrates only slightly more fluorescence than background, as shown in Fig. 3. These results indicate that our molecular beacon design was successful, and that the beacon remained in its stem-loop configuration in the presence of 4 M GuSCN, but that the melting temperature of the beacon was depressed enough that addition of target caused a rapid unfolding, hybridization, and restoration of fluorescence.

Microsystem performance

Using this molecular beacon, we proceeded to detect the presence of 16S rRNA from *E. coli* cells using our microsystem. Cells were introduced into the device through the cell introduction channel (Fig. 1(a)) and trapped by activating the electrodes at 250 Hz and 8 Vpp. After 10 min, the flow was stopped and the PDMS microvalve for the cell introduction channel (Fig. 1(c)) was closed. The cell lysis buffer with 10 nM molecular beacon was introduced through the cell lysis buffer channel (Fig. 1(b)). Upon filling the chamber with cell lysis buffer, all valves were closed, and fluorescence was measured using a laser scanning confocal microscope. Fig. 5 presents the increase of fluorescence of the molecular beacon inside our microchamber as a function of time. The number of trapped cells was calculated to be approximately 50 for this experiment. The fluorescence increases over 20 min to its maximum value and is stable thereafter. This response is slower than the immediate fluorescence increase obtained using an excess of purified DNA oligo target, and we attribute the difference between these two results to inefficiencies in cell lysis. Similar experiments conducted on a standard fluorimeter using *E. coli* cells in the presence of our cell lysis buffer took almost 45 min to reach maximum fluorescence (unpublished results). We suspect that more aggressive cell lysis would result in increased access of the molecular beacon to the rRNA of *E. coli*, and subsequently, increase the hybridization speed as well as

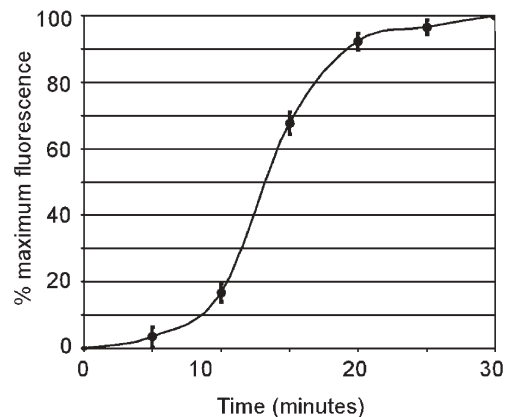


Fig. 5 The hybridization speed of the molecular beacon to complementary rRNA from *E. coli* MC1061 cells in the integrated microsystem. Approximately 50 cells were trapped on the microelectrodes during 10 min of sample flow. The fluorescence rises from background to its maximum over 20 min.

fluorescence maxima, since less rRNA would be degraded by native endonucleases.

Fig. 6 presents a serial dilution of *E. coli* concentrations analyzed using our integrated microsystem. The linear fit to the data demonstrates a linear least-squares regression value of 0.9943 and the extrapolated limit of detection is approximately 25 bacterial cells. This is within the range of clinical utility for detection of pathogenic disease.^{27,28} Further increases in sensitivity may be achieved by lowering the chamber volume and by exciting the molecular beacon with an optimal wavelength (the fluorescence excitation maximum of Rhodamine Red is 568 nm). With these improvements, we expect that a detection limit of 1–3 cells is readily achievable. The maximum enrichment ratio of the cells in this experiment was 160 (16 μL of cells trapped in 100 nL), but in principle, the upper bound of the enrichment factor for a DEP device of this type can be significantly higher and is limited only by the time

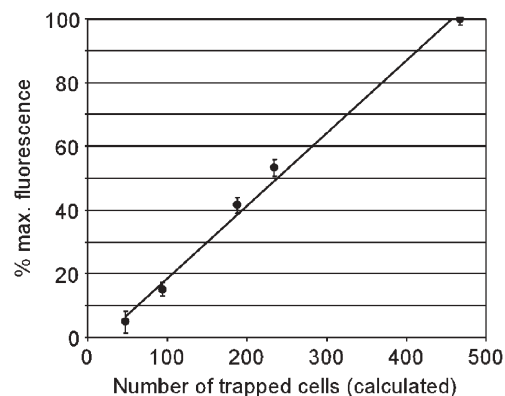


Fig. 6 rRNA detection from lysed *E. coli* cells in the integrated microsystem. Differing concentrations of cells were introduced into the microsystem for 10 min and trapping was performed. The cells were lysed and hybridization was allowed to occur. The linear fit to the data ($R^2 = 0.9943$) indicates that the fluorescence response is linear with cell density. The extrapolated limit of detection is approximately 25 cells.

needed for flowing larger volumes through the device and the surface coverage area of the microelectrodes. In addition, this system is easily amenable to parallelization, and such parallel devices will demonstrate increased volumetric flow rate at lower applied pressures. For example, a 30-chamber device of this type would yield a volumetric flow rate of 3 mL h⁻¹, allowing analysis of standard clinical sample volumes within 30 min.

Conclusions

We present the first work to directly couple a continuous-flow DEP assay for bacterial concentration with room temperature, sequence-specific genetic detection. The microsystem is coupled with a PDMS microvalve system for volume constriction that effectively increases the local detectable concentration of genetic materials. Use of an optical molecular beacon in the presence of high concentrations of a chaotropic salt enables rapid room-temperature laser-induced fluorescence detection of specific genetic sequences. Combining microsystems of this type with other standard molecular biology analysis techniques, such as PCR, will be a natural extension of this work. The resulting ability to couple information about bacterial cell morphology and dielectrophoretic phenotype with genetic information may enable integrated microsystems capable of interrogating cells based on multiple criteria simultaneously.

Acknowledgements

Microdevice fabrication was performed in the UC-Santa Barbara Nanolab. We thank the UC-Santa Barbara College of Engineering Machine Shop for construction of the pneumatic manifolds used in this work, Professor Patrick Daugherty for the *E. coli* MC1061 cells used in these experiments, Dr Paul Bessette for his help with cell culture, and Dr Xiaoyuan Hu for her help with dielectrophoresis theory and device design. The authors also thank Professors C. F. Quate, P. S. Daugherty and K. W. Plaxco for their patient editing of the manuscript. This research was supported by a DARPA/DMEA-CNID award #H94003-05-2-0503 and ARO-ICB award DAAD 19-03-D-0004.

References

- 1 C. F. Edman, P. Mehta, R. Press, C. A. Spargo, G. T. Walker and M. Nerenberg, *J. Invest. Med.*, 2000, **48**, 93–101.
- 2 T. M. H. Lee, M. C. Carles and I. M. Hsing, *Lab Chip*, 2003, **3**, 100–105.
- 3 E. T. Lagally, J. R. Scherer, R. G. Blazej, N. M. Toriello, B. A. Diep, M. Ramchandani, G. F. Sensabaugh, L. W. Riley and R. A. Mathies, *Anal. Chem.*, 2004, **76**, 3162–3170.
- 4 J. J. Gau, E. H. Lan, B. Dunn, C. M. Ho and J. C. S. Woo, *Biosens. Bioelectron.*, 2001, **16**, 745–755.
- 5 Z. Muhammad-Tahir and E. C. Alocilja, *IEEE Sens. J.*, 2003, **3**, 345–351.
- 6 C. G. Koh, W. Tan, M. Q. Zhao, A. J. Ricco and Z. H. Fan, *Anal. Chem.*, 2003, **75**, 4591–4598.
- 7 *Microbial Genome Program Report*, U.S. Department of Energy, 2000.
- 8 J. P. Nataro and J. B. Kaper, *Clin. Microbiol. Rev.*, 1998, **11**, 142.
- 9 C. R. Cabrera and P. Yager, *Electrophoresis*, 2001, **22**, 355–362.
- 10 P. Grodzinski, J. Yang, R. H. Liu and M. D. Ward, *Biomed. Microdev.*, 2003, **5**, 303–310.
- 11 P. R. C. Gascoyne and J. V. Vykoukal, *Proc. IEEE*, 2004, **92**, 22–42.
- 12 R. Holzel, *Biochim. Biophys. Acta*, 1999, 1450.
- 13 R. Pethig and G. H. Markx, *Trends Biotechnol.*, 1997, **15**, 426–432.
- 14 C. Lefevre, H. C. Kang, R. P. Haugland, N. Malekzadeh and S. Arttamangkul, *Bioconjugate Chem.*, 1996, **7**, 482–489.
- 15 T. A. Hall, *Nucleic Acids Symp. Ser.*, 1999, **41**, 95–98.
- 16 L. M. Guzman, D. Belin, M. J. Carson and J. Beckwith, *J. Bacteriol.*, 1995, **177**, 4121–4130.
- 17 W. H. Grover, A. M. Skelley, C. N. Liu, E. T. Lagally and R. A. Mathies, *Sens. Actuators B*, 2003, **89**, 315–323.
- 18 S. Hjerten, *J. Chromatogr.*, 1985, **347**, 191–198.
- 19 C. A. Bopp, F. W. Brenner, P. I. Fields, J. G. Wells and N. A. Strockbine, *Escherichia, Shigella, and Salmonella*, in *Manual of Clinical Microbiology*, ASM Press, Washington, D.C., 2003.
- 20 G. H. Markx, Y. Huang, X. F. Zhou and R. Pethig, *Microbiology*, 1994, **140**, 585–591.
- 21 J. L. McKimmbreschkin, *Virus Res.*, 1992, **22**, 199–206.
- 22 S. C. Tao, Y. Li, Y. H. Liu, X. M. Ma and J. Cheng, *Biotechniques*, 2003, **34**, 1260.
- 23 J. Thompson and D. Gillespie, *Anal. Biochem.*, 1987, **163**, 281–291.
- 24 S. A. E. Marras, F. R. Kramer and S. Tyagi, *Nucleic Acids Res.*, 2002, **30**, e122.
- 25 V. Buschmann, K. D. Weston and M. Sauer, *Bioconjugate Chem.*, 2003, **14**, 195–204.
- 26 R. A. Dalterio, W. H. Nelson, D. Britt and J. F. Sperry, *Appl. Spectrosc.*, 1987, **41**, 234–241.
- 27 L. D. Gray and D. P. Fedorko, *Clin. Microbiol. Rev.*, 1992, **5**, 130–145.
- 28 T. G. Boyce, D. L. Swerdlow and P. M. Griffin, *N. Engl. J. Med.*, 1995, **333**, 364–368.